Published in final edited form as:
Mol Cell. 2010 February 12; 37(3): 370–382. doi:10.1016/j.molcel.2009.12.037.

The connecdenn DENN domain: a GEF for Rab35 mediating cargo-specific exit from early endosomes

Patrick D. Allaire[1], **Andrea L. Marat**[1], **Claudia Dall'Armi**[2], **Gilbert Di Paolo**[2], **Peter S. McPherson**[1,*], and **Brigitte Ritter**[1,*]

[1]Department of Neurology and Neurosurgery, Montreal Neurological Institute, McGill University, Montreal, Quebec H3A 2B4, Canada

[2]Department of Pathology and Cell Biology, Taub Institute for Research on Alzheimer's Disease and the Aging Brain, Columbia University Medical Center, College of Physicians and Surgeons, 630 West 168th Street, New York, New York 10032, USA

Summary

The DENN domain is an evolutionarily ancient protein module. Mutations in the DENN domain cause developmental defects in plants and human diseases, yet the function of this common module is unknown. We now demonstrate that the connecdenn DENN domain functions as a guanine nucleotide exchange factor for Rab35 to regulate endosomal trafficking. Loss of Rab35 activity causes an enlargement of early endosomes, inhibits MHCI recycling, and prevents the early endosomal recruitment of EHD1, a common component recycling tubules on endosomes. Our data are the first to reveal an enzymatic activity for a DENN domain and demonstrate that distinct Rab GTPases can recruit a common protein machinery to various sites within the endosomal network to establish cargo-selective recycling pathways.

Introduction

Cargo molecules entering eukaryotic cells in either clathrin-dependent or -independent carriers are delivered to early endosomes from where they can be sorted for recycling back to the plasma membrane (PM), either directly or following delivery to recycling endosomes. The functional control of these pathways depends on Rab GTPases. Rabs oscillate between active GTP-bound and inactive GDP-bound states via the actions of guanine nucleotide exchange factors (GEFs) and GTPase activating proteins (GAPs). Once activated, Rabs recruit effectors that control endosomal trafficking activities including vesicle formation and transport as well as tethering and fusion. Further complexity results from the fact that multiple Rabs can co-exist on a single endosome, increasing the variety of sorting decisions available (Kouranti et al., 2006; Magadan

*address correspondence to: Dr. Peter S. McPherson, Department of Neurology and Neurosurgery, Montreal Neurological Institute, McGill University, 3801 University Street, Montreal, QC H3A 2B4, Canada, phone: (514) 398-7355, fax: (514) 398-8106, peter.mcpherson@mcgill.ca, Dr. Brigitte Ritter, Department of Neurology and Neurosurgery, Montreal Neurological Institute, McGill University, 3801 University Street, Montreal, QC H3A 2B4, Canada, phone: (514) 398-6644 ext. 00209, fax: (514) 398-8106, brigitte.ritter@mcgill.ca.

The authors declare no competing financial interests.

et al., 2006; Simpson et al., 2004; Sonnichsen et al., 2000). To date, only a few Rabs have been matched to their GEFs and GAPs, hampering a better understanding of their function.

Rab35, a recently characterized Rab functions in endosomal trafficking (Kouranti et al., 2006; Patino-Lopez et al., 2008; Sato et al., 2008; Walseng et al., 2008). Rab35 localizes to the PM and to internal vesicles and tubules and is required for endosomal secretion during immunological synapse formation and for stabilization and successful abscission of the cytokinesis bridge (Kouranti et al., 2006; Patino-Lopez et al., 2008). Additionally, Rab35 is linked to actin dynamics during neurite outgrowth and to actin bundling during bristle formation in *Drosophila* (Chevallier et al., 2009; Zhang et al., 2009). It has also been linked to the recycling of transferrin and major histocompatibility complex class II (MHCII), which use clathrin-dependent and-independent internalization pathways, respectively (Kouranti et al., 2006; Walseng et al., 2008). MHCII recycling involves the formation of Rab35/EHD1-positives tubules on early endosomes (Walseng et al., 2008). At recycling endosomes, Rab11/EHD1 tubules recycle transferrin while MHC class I (MHCI) and β1-integrin are sorted into Rab22/EHD1 tubules (Caplan et al., 2002; Naslavsky et al., 2004a; Naslavsky et al., 2003; Naslavsky et al., 2004b; Weigert et al., 2004). EHD1/Rme-1 is the founding member of the EHD protein family that in mammals comprises four members (reviewed in Grant and Caplan, 2008). EHD proteins form homo- and heterooligomers and function in the formation of intracellular transport carriers (Blume et al., 2007; Daumke et al., 2007).

We identified connecdenn as a component of clathrin-coated vesicles (CCVs) and demonstrated that connecdenn knock-down (KD) alters synaptic vesicle recycling in cultured neurons (Allaire et al., 2006). Interestingly, connecdenn remains on CCV membranes after clathrin coat removal, indicative of a post-uncoating function (Allaire et al., 2006). The connecdenn N-terminus harbors a Differentially Expressed in Neoplastic versus Normal cells (DENN) domain, formed by upstream DENN (uDENN), DENN, and downstream DENN (dDENN) modules. DENN domains are found in 16 human genes and mutations in DENN domains and DENN domain proteins cause human disease (Azzedine et al., 2003; Del Villar and Miller, 2004; Lichy et al., 1992; Senderek et al., 2003; Volterra and Meldolesi, 2005), yet the function of the domain remains elusive. We now demonstrate that the connecdenn DENN domain is a lipid-binding module both necessary and sufficient for the stable membrane association of connecdenn with uncoated CCVs. Importantly, the DENN domain binds Rab35 and functions as a GEF for this GTPase. KD of connecdenn or Rab35 disrupts recruitment of EHD1 to early endosomes and leads to an enlargement of the compartment. Moreover, loss of function studies reveal that Rab35 controls recycling of MHCI but not β1-integrin or transferrin from early endosomes. Our data thus highlight that distinct Rab GTPases recruit a common protein machinery to various sites within the endosomal network to establish distinct endosomal recycling pathways that are utilized by specific subsets of cargo.

Results

The DENN domain positions connecdenn for a post-endocytosis function

Connecdenn has an exceptionally stable association with the membrane fraction of uncoated CCVs (Allaire et al., 2006; Fig. S1A). To identify the responsible molecular determinant, we tested Flag-tagged variants of full-length connecdenn, the C-terminal region lacking the DENN domain and the isolated DENN domain (Fig. 1A) for their ability to target to CCVs in transfected cells. Flag-tagged full-length connecdenn enriched on isolated CCVs and remained on stripped vesicles similar to the endogenous protein (Fig. 1B/C, Fig. S1A). The C-terminal region also enriched on CCVs (Fig. 1B), likely through interactions with AP-2, a coat protein that binds connecdenn (Allaire et al., 2006). However, this construct was readily extracted, suggesting that the DENN domain, which alone does not target to CCVs, mediates membrane stability (Fig. 1B/C). This was verified by fusing the DENN domain to the C-terminal region

of NECAP 1, a CCV protein that targets CCVs through its C-terminal region but that efficiently strips off vesicles (Ritter et al., 2003, Fig. 1D). Importantly, the chimeric DENN/NECAP protein not only targeted to CCVs but remained on the vesicles following coat removal (Fig. 1D).

To better understand this association, we tested the isolated DENN domain for lipid binding using sedimentation assays. The DENN domain displayed a broad spectrum of lipid interactions (Fig. 1E), likely explaining the membrane stability. In respect to phosphatidylinositol-phosphates (PtdInsP), which help create the specificity of organellar membranes, the DENN domain showed a slight preference for PtdIns(3)P (Fig. 1E). However, since the domain interacts broadly with PtdInsPs, it is unlikely that the DENN domain determines to which membranes connecdenn will target. As such, connecdenn may be initially recruited to CCVs through C-terminal interactions with coat proteins while the lipid binding of the DENN domain aids in increased membrane stability during vesicle maturation, allowing for a subsequent post-endocytosis function.

A post-uncoating role for connecdenn was also demonstrated by a study in *C. elegans* (Sato et al., 2008). RME-5, the *C. elegans* ortholog of Rab35 was shown to depend on RME-4, the *C. elegans* ortholog of connecdenn for CCV-dependent transport to endosomes in oocytes (Sato et al., 2008). Impairment of either protein led to defects in yolk receptor recycling (Sato et al., 2008). RME-4 binds the GDP-bound form of RME-5/Rab35, yet the mechanism of RME-5/Rab35 activation remains unclear (Sato et al., 2008). To clarify the connecdenn/Rab35 relationship, we tested if Rab35 is also a component of CCVs. Like Rab5, Rab35 is present on CCVs (Fig. 2A) although neither protein shows the same enrichment as AP-2 and connecdenn (Fig. 2A). Early endosome antigen 1 (EEA1) is excluded from the CCV fraction, indicating that the presence of the Rabs is not due to early endosome contamination (Fig. 2A). Rab35 also co-migrates with CCVs on a continuous sucrose gradient (Fig. 2B). In COS-7 cells, a pool of Rab35 localizes to forming CCVs at the PM (Fig. 2C). Thus, connecdenn and Rab35 are both present on CCVs.

The connecdenn DENN domain binds Rab35 and functions as a GEF

Full-length connecdenn binds Rab35 and importantly, the isolated DENN domain is fully responsible for binding (Fig. 3A). Binding increases with EDTA (Fig. 3A), which chelates Mg^{2+} and destabilizes the interaction of guanine nucleotides with GTPases. In addition, purified GST-DENN domain affinity-selected wild-type (wt) Rab35 (Fig. 3B). Even stronger binding was seen with Rab35 S22N, which reduces nucleotide affinity analogous to Ras S17N and no binding was observed to Rab35 Q67L, a mutation that impairs GTP hydrolysis keeping the protein in a GTP-bound state (Fig. 3B). There was no binding of the DENN domain to endosomal Rabs 4, 5, and 11 under nucleotide-free conditions (Fig. 3E). Flag-tagged connecdenn co-localized with Rab35 S22N in punctate structures while little co-localization was observed with Rab35 Q67L (Fig. 3C). Moreover, co-immunoprecipitation studies using GFP-tagged Rab35 wt, S22N or Q67L revealed that the inactive variant efficiently co-immunoprecipitates endogenous connecdenn (Fig. 3D). Together, these data demonstrate that the connecdenn DENN domain forms a specific interaction with the inactive form of Rab35.

Preference for the inactive form is a signature of GEFs. We thus tested the DENN domain for GEF activity and indeed, the purified domain efficiently facilitates the exchange of GDP for GTP on Rab35 (Fig. 3F). In 3 minutes at room temperature, 1.5 pmoles of DENN domain allowed for loading of 17.4 (±0.9) pmoles GTP onto 18.7 pmoles of Rab35 pre-loaded with GDP, thus yielding nucleotide exchange on 93% of Rab35 (Fig. 3F). In contrast, the DENN domain showed no activity for Rab3 or Rab5 and there was little activity with Rab35 alone (Fig. 3F). Moreover, the isolated DH/PH domain of intersectin, a potent GEF for Cdc42 (Hussain et al., 2001) does not promote GTP-loading of Rab35 (Fig. 3F). In comparison, 1.5

pmoles of purified GEF domain from Rabex5 (aa 1-399, Zhu et al., 2007) exchange 3.3 (±0.2) pmoles of GDP for GTP on 18.7 pmoles of Rab5 over 3 minutes (Fig. 3F/G). This activity is best seen when plotted on an expanded scale, which also reveals that Rabex5 has no activity towards Rab35 and that the DENN domain of connecdenn has no activity towards Rab5 (Fig. 3G). The ability of the DENN domain to retain connecdenn on uncoated CCVs and to function as a Rab35 GEF likely provides a means to activate Rab35 while the vesicles enter the endosomal system.

Connecdenn and Rab35 KD cause enlargement of early endosomes

To analyze the functional consequences of DENN domain-mediated Rab35 activation, we performed loss of function studies in COS-7 cells, a line with high levels of endogenous connecdenn (Fig. S1B). Lentiviral delivery of GFP reporter constructs that also encode synthetic small hairpin RNA sequences within the context of a microRNA (shRNAmiR) for KD of Rab35 or connecdenn led to efficient reductions in both proteins (Fig. 4A). Connecdenn levels were reduced to approximately 2 and 9% of control using shRNAmiRs CD nt248 and CD nt275, respectively, whereas Rab35 was reduced to 41 and 46% using shRNAmiRs Rab35 nt63 and Rab35 nt419, respectively (Fig. 4A). Interestingly, connecdenn levels were slightly reduced following Rab35 KD. Together with the selective co-localization and co-immunoprecipitation of connecdenn with inactive Rab35 (Fig. 3 C/D), this suggests that connecdenn and inactive Rab35 form in part, a steady state complex, which may provide a reservoir of Rab35 to be activated on demand. Removal of Rab35 could thus destabilize connecdenn. In contrast, KD of either connecdenn or Rab35 had no apparent influence on clathrin-heavy chain, EEA1, and Rab11 (Fig. 4A).

Rab35 KD had no obvious influence on the distribution of the clathrin adaptors AP-1 and AP-2 or on the recycling endosome protein Rab11 (Fig. 4B, Fig. S2), whereas it caused an enlargement of Rab5- and EEA1-positive early endosomes, which in most cases clustered in the peri-nuclear region (Fig. 4A/B, Fig. S2). Importantly, the Rab35 and connecdenn KD phenotypes were essentially identical (Fig. 4B, Fig. S2), indicating that connecdenn through its DENN domain is a key regulator of Rab35 activity.

Through an unknown mechanism, Rab5 levels were increased following Rab35 or connecdenn KD (Fig. 4A). Rab5 and PtdIns(3)P recruit EEA1 to endosomal membranes. EEA1 is required for homotypic fusion of endocytic vesicles and for their fusion with early endosomes (Hoepfner et al., 2005;Nielsen et al., 1999;Simonsen et al., 1998;Zerial and McBride, 2001). The enlargement of early endosomes could thus reflect an enhanced fusion caused by Rab5 up regulation. However, early endosomes not only receive a constant flow of newly endocytosed material but continually relay cargo to recycling and degradative routes. Thus, enlargement of this compartment could alternatively be attributed to a block in an exit route.

Rab35 activiation is required for cargo-selective recycling from early endosomes

Rab35 is linked to the recycling of both clathrin-dependent and -independent cargo. Over expression of dominant-negative Rab35 S22N was reported to impair recycling of transferrin at early time points, suggesting a function in fast transferrin recycling from early endosomes. (Kouranti et al., 2006). Surprisingly, however, we detected no significant differences in the kinetics of transferrin endocytosis (Fig. 5A-C) or recycling (Fig. 5A/D) by flow cytometry or using densitometry to quantify the amount of fluorescent transferrin that remains in control and KD cells at various time points after loading and chase (Fig. S3A/B). We also failed to detect significant kinetic defects for transferrin recycling rates following over expression of GFP-tagged Rab35 variants in COS-7 and HeLa cells (Fig. S3C/D). Together, our data do not indicate a major role for connecdenn and Rab35 in transferrin recycling.

Specific clathrin-independent cargo follow at least two distinct itineraries upon internalization and delivery to endosomes. EHD1-positive tubules recycle MHCII from early endosomes and MHCI and β1-integrin from recycling endosomes (Walseng et al., 2008; Weigert et al., 2004). When examining MHC recycling, we observed that following a 20 min pulse, labeled MHCI localized in part to EEA1-positive early endosomes in control and KD cells (Fig. 6A, Fig. S4). In KD cells, MHCI was found in the enlarged endosomes that had relocalized to the perinuclear region (Fig. 6A, Fig. S4). Along with the observations on transferrin, these data demonstrate that the change in size and localization of EEA1 endosomes in the KD cells does not affect their ability to receive cargo. However, following a 20 min chase, significantly higher amounts of MHCI were retained in the KD cells compared to control (Fig. 6B), revealing that DENN-domain mediated activation of Rab35 is necessary for efficient trafficking of MHCI following its delivery to EEA1-positive early endosomes.

In control cells following a 20 min pulse, MHCI is readily detected in recycling tubules decorated with EHD1 (Fig. 6C). A large number of these tubules originate from EEA1-positive early endosomes (Fig. 6D, Fig. S5). Triple labeling with GFP-tagged Rab35 and myc-tagged EHD1 reveal pools of these proteins on EEA1-positive endosomes (Fig. 6E), suggesting that Rab35 could control the recruitment of EHD1 to early endosomes for cargo recycling. Consistently, connecdenn and Rab35 KD cause EHD1 to redistribute into the cytosol and lead to a reduction in tubule formation (Fig. 6D, Fig. S5). Together, our data demonstrate that connecdenn and Rab35 control the recycling of specific cargo from early endosomes. Thus, the endosome enlargement observed upon connecdenn or Rab35 KD is likely due to a block of at least one exit route out of early endosomes.

To further examine the relationship of Rab35 to Rab5 in terms of early endosome enlargement, we expressed Rab5 alone or with Rab35 S22N. Expression of Flag-Rab35 S22N with GFP-Rab5 caused the appearance of enlarged early endosomes that were similar to those seen with expression of constitutively active GFP-Rab5 Q79L alone (Fig. 7A). In contrast, expression of wt Rab5 alone did not lead to early endosome enlargement (Fig. 7A). Thus, inactivation of Rab35 through KD, KD of its GEF, or expression of inactive Rab35 is sufficient to cause early endosome enlargement. More importantly, the early endosome phenotype seen in connecdenn KD cells is rescued with active GFP-Rab35 (Q67L) but not GFP alone (Fig. 7B/C). This supports the notion that Rab35 activity is required to establish an early endosomal exit route and that its disruption leads to an increase in the size of the donor compartment.

To better understand if the recycling phenotype is caused by the lack of active Rab35 or increased expression of Rab5, we analyzed MHCI recycling in cells expressing Rab5 wt alone, active Rab5 (Q79L) alone, or Rab5 together with its GEF Rabex5. Interestingly, each condition showed a small but significant increase in the efficiency of MHCI recycling compared to cells expressing GFP alone (Fig. 7D/E). This is opposite of what is observed upon connecdenn or Rab35 KD (Fig. 6B), suggesting that the Rab5 upregulation is not responsible for the decrease in MHCI recycling. Together, these experiments support that both the early endosomal enlargement and the MHCI recycling defect are direct consequences of the loss of Rab35 activity. The slight increase in MHCI recycling seen with elevated Rab5 levels could indicate that under KD conditions, cells up regulate Rab5 in an attempt to compensate for the trafficking defect, though the trafficking route involved remains unknown.

In summary, we demonstrate that connecdenn-activated Rab35 controls the formation of EHD1-positive recycling tubules from early endosomes, similar to the function attributed to Rab11 and Rab22 at recycling endosomes. Interestingly, this trafficking route appears to be cargo-specific. β1-integrin also uses the canonical MHCI transport pathway from early to recycling endosomes for Rab22/EHD1-mediated recycling to the plasma membrane. Using flow cytometry, we did not detect any significant differences in β1-intergin recycling between

connecdenn or Rab35 KD and control cells (Fig. S3), similar to the lack of trafficking defects we observed for transferrin. This demonstrates that Rab35 and its GEF connecdenn provide a means to promote the recycling of a specific subset of cargo from early endosomes.

Discussion

DENN domains are found in multiple protein products encoded by 16 human genes including myotubularin related (MTMR) 5 and 13, DENN/MADD, suppressor of tumorgenicity 5, Rab6-interacting protein 1 (Rab6IP1), connecdenn, and a number of uncharacterized proteins. The presence of a single DENN domain protein in *Schizosaccharomyces pombe* indicates that the DENN domain is evolutionary ancient and bioinformatics suggests it is present in all eukaryotes (Harsay and Schekman, 2007). Mutations in DENN domains and their parent proteins cause human diseases (Azzedine et al., 2003; Del Villar and Miller, 2004; Lichy et al., 1992; Senderek et al., 2003; Volterra and Meldolesi, 2005). Notably, Charcot-Marie-Tooth 4B2 neuropathy is caused by deletion of the dDENN in MTMR 13 (Senderek et al., 2003). Even in *Arabidopsis thaliana*, a point mutation in the DENN domain of SCD1 impairs exocytic vesicle trafficking crucial for cytokinesis and polarized cell expansion and causes sterility (Falbel et al., 2003). Thus, DENN domain proteins mediate crucial functions throughout evolution.

In several cases, DENN domain proteins have been linked to Rabs but no common mode of interaction has been gleaned. Rab6IP1 binds to Rab6 and Rab11 in their GTP-bound form but also binds GDP-bound Rab6 (Miserey-Lenkei et al., 2007). DENN/MADD selectively binds through its uDENN to GTP-bound Rab3 (Niwa et al., 2008). However, DENN/MADD also functions as a GEF for Rab3 (Wada et al., 1997). Notably, the GEF activity has only been observed with full-length protein and it is argued that the GEF activity resides outside of the DENN domain (Coppola et al., 2002). We now demonstrate that the purified connecdenn DENN domain has intrinsic GEF activity specific for Rab35. Our study is the first to assign an enzymatic activity to the DENN domain and it will be interesting to see if other DENN domains function as GEFs towards other Rabs.

We propose a model for connecdenn function in which the protein is recruited to nascent CCVs through C-terminal interactions with AP-2 while the DENN domain anchors the protein to the vesicle membrane and functions as a platform for Rab35 recruitment. Transition of the endocytic carrier from PtdIns(4,5)P_2 to PtdIns(3)P, the PtdInsP enriched on endocytic vesicles could signal to the DENN domain to exert its GEF function. Connecdenn would then dissociate from the vesicle before fusion with EEA1-positive endosomes and in fact, we observe minimal co-localization of connecdenn and EEA1 (data not shown). Activated Rab35 remains on the vesicles for delivery to early endosomes, where its effector protein(s) control the recruitment of EHD1 for cargo recycling.

Over expression studies have linked Rab35 to the fast transferrin recycling pathway from early endosomes to the PM (Kouranti et al., 2006), a function previously assigned to Rab4 (Daro et al., 1996; van der Sluijs et al., 1992). However, Deneka et al. (2003) showed that KD of Rab4 enhanced transferrin recycling and our studies reveal that Rab35 KD does not affect transferrin trafficking. Thus, the Rab-based protein machinery for this transport pathway is yet to be defined.

KD of Rab35 and connecdenn impairs recycling of MHCI. MHCI is internalized in a clathrin-independent pathway that merges with EEA1-positive endosomes (Naslavsky et al., 2003). From there, MHCI is either delivered to late endosomes/lysosomes or traffics to recycling endosomes for recycling back to the PM in transferrin-negative, Rab22-positive tubular structures (Weigert et al., 2004). In addition, these tubules contain Rab11 and EHD1, which

also regulate the recycling of clathrin-dependent cargo from recycling endosomes (Caplan et al., 2002; Grant et al., 2001; Lin et al., 2001; Weigert et al., 2004). Clathrin-independent and -dependent cargo thus utilize in part common machineries to recycle from recycling endosomes to the PM (Weigert et al., 2004). Weigert et al. (2004) further describe MHCI-positive tubules that originate from transferrin-positive endosomal structures but the protein machinery involved in their formation remained undefined. Our studies demonstrate that Rab35 activation is crucial for EHD1 recruitment to EEA1-positive endosomes and for efficient MHCI recycling. Together, these data suggest that MHCI recycling from distinct intracellular locations is likely mediated by a common protein machinery but that the spatial organization of this machinery is determined by pathway-specific Rab GTPases. Moreover, these pathways seem, at least in part, to be cargo-specific. β1-integrin has been shown to follow the MHCI trafficking route from the PM to recycling endosomes and back (Jovic et al., 2009; Jovic et al., 2007; Powelka et al., 2004), however, KD of Rab35 or connecdenn does not impair the trafficking of this cargo. This is reminiscent of recent data from the Corvera group, which demonstrated differences in the early endosomal processing of endocytic vesicles dependent on the cargo they carried (Leonard et al., 2008). Incoming transferrin is efficiently routed to recycling endosomes whereas EGF is retained in EEA1-positive endosomes for delivery to the degradative pathway due to higher levels of Rab5 present on EGF-delivering vesicles (Leonard et al., 2008), underscoring the importance of Rabs for sorting decisions within the endosomal network.

In summary, our results reveal an enzymatic activity for a DENN domain and given the ancient nature of this module, it is likely that this activity functions broadly throughout eukaryotes. Moreover, our results indicate that distinct Rabs GTPases use a common protein machinery to control cargo selective recycling from different sites in the endosomal system.

Experimental Procedures

Antibodies and reagents, protein and lipid binding assays, virus production and KD conditions

These procedures are described in the Supplemental Material.

Subcellular fractionation

CCVs were purified from adult rat brain or cell lines in buffer A (100 mM MES, pH 6.5, 1 mM EGTA and 5 mM $MgCl_2$) as described (Girard et al., 2005). For the extraction of coat proteins, 50-100 μg aliquots of CCVs were suspended in 100 μl of buffer A or 0.5 M Tris pH 8.0 EDTA (1:1 buffer A and 1 M Tris pH 9.0) and incubated for 30 min on ice. The samples were centrifuged at 200,000 x*g* to separate coats (supernatant) and stripped vesicles (pellet). CCVs were further separated on linear 20–50% sucrose gradients as described (Girard et al., 2005).

Purification and cleavage of fusion proteins

GST fusion proteins were expressed in BL21 bacteria and purified using standard procedures. pEBG constructs for expression of GST-tagged fusion proteins in mammalian cells were transfected into HEK 293-T cells using calcium phosphate. After 48 hours, cells were scraped in PBS buffer with protease inhibitors (0.83 mM benzamidine, 0.23 mM phenylmethylsulphonyl fluoride, 0.5 μg/ml aprotinin and 0.5 μg/ml leupeptin), lysed by sonication, Triton X-100 was added to 1% final and cells were spun at 205,000 x*g* for 30 min before purification of the fusion protein on glutathione-Sepharose beads.

For GDP/GTP exchange assays, GST tags were removed by incubating the fusion proteins bound to glutathione-Sepharose in thrombin cleavage buffer (50 mM Tris, pH 8.0, 150 mM

NaCl, 5 mM $MgCl_2$, 1 mM DTT), overnight at 4°C using 5 units of thrombin (Sigma, St-Louis, USA) in 500 μl total volume. Thrombin was cleared with benzamidine-Sepharose (GE Healthcare, Chalfont St. Giles, United Kingdom) and the supernatant was exchanged into appropriate buffer and concentrated using a Millipore Amicon Ultra-15 filter (Millipore, Carrintwohill, Ireland). For GST affinity selection assays, all GST fusion proteins were expressed in BL21 with the exception of the connecdenn DENN domain, which was purified from HEK 293-T cells. All proteins used in GDP/GTP exchange assays were expressed in HEK 293-T cells except for GST-DH/PH and GST-Rabex5 (aa1-399), which were expressed in BL21.

GDP/GTP exchange assay

GST-cleaved Rab3, Rab5, and Rab35 were exchanged into GEF loading buffer (20 mM Tris pH 7.5, 100 mM NaCl) and Rabex5 (aa1-399) and the DENN domain were exchanged into GEF incubation buffer (20 mM Tris pH 7.5, 100 mM NaCl and 5 mM $MgCl_2$). Purified GTPases (15 M) were loaded with 40 μM GDP by incubation at 30°C for 10 min in GEF loading buffer containing 5 mM EDTA. Loaded GDP was stabilized by the addition of 10 mM $MgCl_2$. Exchange reactions were carried out at room temperature in 130 μl total volume containing 1.25 μM loaded GTPase, 100 nM DENN domain or Rabex5 (aa1-399), 0.5 mg/ml BSA, 5 μM GTPγS, 0.2 mCi/mmol [^{35}S]GTPγS, and 0.5 mM DTT in GEF incubation buffer. At the indicated times, 15 μl of the reaction were removed, added to 1ml of ice cold wash buffer (20 mM Tris pH 7.5, 100 mM NaCl, 20 mM $MgCl_2$), passed through nitrocellulose filters, washed with 5 ml wash buffer and counted using a liquid scintillation counter (Beckmann Coulter LS6500 Scintillator). For the plots, background signals from samples at time 0 (before addition of the Rabs) were subtracted from the values obtained at the subsequent time points.

Immunofluorescence

COS-7 cells were plated on poly-L-lysine-coated coverslips and transfected using Lipofectamine 2000 (Invitrogen) the next day. Transduced cells were transfected using jetPRIME (Polyplus Transfection) according to the manufacturer's recommendations or using Lipofectamine 2000, limiting the incubation time with the Lipofectamine 2000/DNA mix to 60 min. Following overnight incubation, cells were fixed in 4% PFA and processed for immunofluorescence following standard protocols. For the localization of marker proteins, KD cells were plated one to two days before analysis and processed for immunofluorescence on day five after transduction. For the rescue of the EEA1 KD phenotype, cells transduced with RFP control virus or RFP-tagged viruses for KD of connecdenn or Rab35 were plated on coverslips three days after transduction, transfected with GFP alone or GFP-Rab35 Q67L on day 4 after transduction using jetPRIME, and processed for immunofluorescence five days after transduction. Images were taken without selecting for the state of the EEA1 signal and pictures were analyzed blind to determine the persistence of the EEA1 KD phenotype in GFP-positive cells. For MHCI recycling, cells were incubated with 1 μg of antibody per 10^6 cells for 20 min at 37°C in culture medium. The cells were chilled on ice and surface-bound antibody was removed by acid wash (0.2M acetic acid, 0.5M NaCl) followed by a PBS wash, and the cells were fixed and processed as described above.

Endocytosis and recycling assays

For transferrin internalization assays, cells were starved in DMEM overnight and analyzed on day five after transduction. The cells were chilled on ice for 30 min and then incubated with Alexa633-transferrin (200 μ g/ml) in ice-cold DMEM on ice for 60 min. Cells were washed with cold PBS and incubated in pre-warmed culture medium at 37°C for various times. At each time point, a sample of cells was chilled on ice, surface-bound transferrin was removed by acid wash followed by a PBS wash. The cells were removed from the plate in 1 ml of PBS by

pipetting, filtered through a cell strainer and analyzed in by flow cytometry on a FACSCalibur (Becton Dickinson). For transferrin recycling assays using transduced cells or cells transfected for 2 or 3 days, cells were serum starved overnight and incubated with Alexa633-transferrin for 60 min at 37°C. Surface-bound transferrin was removed on ice by acid wash, followed by a PBS wash. The cells were then incubated in pre-warmed culture medium at 37°C for the times indicated and processed for flow cytometry as described above. Due to lower expression levels of GFP-Rab35 S22N, transfected cells were gated in the GFP channel such that all cells analyzed had a fluorescence intensity of 10 arbitrary units or more. For the immunofluorescence-based recycling assay, cells were serum starved overnight, incubated with Cy3-labeled transferrin for 1 hr at 16°C, and acid washed on ice, followed by a PBS wash. The cells were then incubated in pre-warmed culture medium at 37°C for the times indicated. At each time point, a sample of cells was acid washed on ice, fixed in 2% PFA and fields of cells were chosen for imaging solely based on the GFP channel. Internal transferrin amounts were then quantified measuring the transferrin signal intensity of cells located completely within the fields using ImageJ (Rasband, W.S., ImageJ, U. S. National Institutes of Health, Bethesda, Maryland, USA, http://rsb.info.nih.gov/ij/, 1997-2008).

For MHCI recycling assays, two sets of transduced or transfected cells were incubated with 1 μg of antibody per 10^6 cells for 20 min at 37°C in culture medium. Both sets were chilled on ice and surface-bound antibody was removed by acid wash, followed by a PBS wash. The second set was then incubated in pre-warmed culture medium at 37°C for 20 min, chilled on ice and surface-bound antibody was removed by acid wash, followed by a PBS wash. Both sets were fixed in 2% PFA, permeabilized with 0.2% Triton X-100 in PBS and incubated with Alexa647-conjugated secondary antibodies for 30 min on ice. The cells were washed with PBS, scraped off the plates and processed by flow cytometry. For the co-expression of GFP-Rab5 with myc-tagged Rabex5, a DNA ratio of 1:4 (Rab5:Rabex) was used to ensure that the majority of Rab5-positive cells also express Rabex5. For β1-integrin recycling assays, two sets of cells were starved in DMEM for 1 hour at 37°C, incubated with 1 μg of antibody per 10^6 cells for 2 h at 37°C in DMEM, chilled on ice and surface-bound antibody was removed by acid wash, followed by a PBS wash. The second set was then incubated in pre-warmed culture medium at 37°C for 2 h, acid washed on, followed by a PBS wash. Both sets were fixed in 2% PFA, permeabilized with 0.2% Triton X-100 in PBS and incubated with Alexa647-conjugated secondary antibodies for 30 min on ice. The cells were then washed with PBS and processed by flow cytometry. In each assay, 10,000 cells were analyzed for each time point and condition.

Supplementary Material

Refer to Web version on PubMed Central for supplementary material.

Acknowledgments

We thank Drs. Steve Caplan, John Presley, and Juan Bonifacino for reagents, Jacynthe Philie and Lyne Bourbonniere for technical assistance, and Dr. Viviane Poupon for helpful discussions and assistance with the flow cytometry assays. This research was supported by Canadian Institutes of Health Research (CIHR) grant MOP-13461 to PSM. ALM was supported by a Fonds de la recherche en santé du Québec (FRSQ) fellowship. PSM is a FRSQ Senior Scholar and holds the James McGill Chair. GDP is funded by NIH grant R01 NS056049.

References

Allaire PD, Ritter B, Thomas S, Burman JL, Denisov AY, Legendre-Guillemin V, Harper SQ, Davidson BL, Gehring K, McPherson PS. Connecdenn, a novel DENN domain-containing protein of neuronal clathrin-coated vesicles functioning in synaptic vesicle endocytosis. J Neurosci 2006;26:13202–13212. [PubMed: 17182770]

Azzedine H, Bolino A, Taieb T, Birouk N, Di Duca M, Bouhouche A, Benamou S, Mrabet A, Hammadouche T, Chkili T, et al. Mutations in MTMR13, a new pseudophosphatase homologue of MTMR2 and Sbf1, in two families with an autosomal recessive demyelinating form of Charcot-Marie-Tooth disease associated with early-onset glaucoma. Am J Hum Genet 2003;72:1141–1153. [PubMed: 12687498]

Blume JJ, Halbach A, Behrendt D, Paulsson M, Plomann M. EHD proteins are associated with tubular and vesicular compartments and interact with specific phospholipids. Exp Cell Res 2007;313:219–231. [PubMed: 17097635]

Caplan S, Naslavsky N, Hartnell LM, Lodge R, Polishchuk RS, Donaldson JG, Bonifacino JS. A tubular EHD1-containing compartment involved in the recycling of major histocompatibility complex class I molecules to the plasma membrane. Embo J 2002;21:2557–2567. [PubMed: 12032069]

Chevallier J, Koop C, Srivastava A, Petrie RJ, Lamarche-Vane N, Presley JF. Rab35 regulates neurite outgrowth and cell shape. FEBS Lett 2009;583:1096–1101. [PubMed: 19289122]

Coppola T, Perret-Menoud V, Gattesco S, Magnin S, Pombo I, Blank U, Regazzi R. The death domain of Rab3 guanine nucleotide exchange protein in GDP/GTP exchange activity in living cells. Biochem J 2002;362:273–279. [PubMed: 11853534]

Daro E, van der Sluijs P, Galli T, Mellman I. Rab4 and cellubrevin define different early endosome populations on the pathway of transferrin receptor recycling. Proc Natl Acad Sci U S A 1996;93:9559–9564. [PubMed: 8790369]

Daumke O, Lundmark R, Vallis Y, Martens S, Butler PJ, McMahon HT. Architectural and mechanistic insights into an EHD ATPase involved in membrane remodelling. Nature 2007;449:923–927. [PubMed: 17914359]

Del Villar K, Miller CA. Down-regulation of DENN/MADD, a TNF receptor binding protein, correlates with neuronal cell death in Alzheimer's disease brain and hippocampal neurons. Proc Natl Acad Sci U S A 2004;101:4210–4215. [PubMed: 15007167]

Deneka M, Neeft M, Popa I, van Oort M, Sprong H, Oorschot V, Klumperman J, Schu P, van der Sluijs P. Rabaptin-5alpha/rabaptin-4 serves as a linker between rab4 and gamma(1)-adaptin in membrane recycling from endosomes. Embo J 2003;22:2645–2657. [PubMed: 12773381]

Falbel TG, Koch LM, Nadeau JA, Segui-Simarro JM, Sack FD, Bednarek SY. SCD1 is required for cytokinesis and polarized cell expansion in Arabidopsis thaliana [corrected]. Development 2003;130:4011–4024. [PubMed: 12874123]

Girard M, Allaire PD, Blondeau F, McPherson PS. Isolation of clathrin-coated vesicles by differential and density gradient centrifugation. Curr Protoc Cell Biol. 2005;Chapter 3(Unit 3):13.

Grant B, Zhang Y, Paupard MC, Lin SX, Hall DH, Hirsh D. Evidence that RME-1, a conserved C. elegans EH-domain protein, functions in endocytic recycling. Nat Cell Biol 2001;3:573–579. [PubMed: 11389442]

Grant BD, Caplan S. Mechanisms of EHD/RME-1 protein function in endocytic transport. Traffic 2008;9:2043–2052. [PubMed: 18801062]

Harsay E, Schekman R. Avl9p, a member of a novel protein superfamily, functions in the late secretory pathway. Mol Biol Cell 2007;18:1203–1219. [PubMed: 17229886]

Hoepfner S, Severin F, Cabezas A, Habermann B, Runge A, Gillooly D, Stenmark H, Zerial M. Modulation of receptor recycling and degradation by the endosomal kinesin KIF16B. Cell 2005;121:437–450. [PubMed: 15882625]

Hussain NK, Jenna S, Glogauer M, Quinn CC, Wasiak S, Guipponi M, Antonarakis SE, Kay BK, Stossel TP, Lamarche-Vane N, McPherson PS. Endocytic protein intersectin-l regulates actin assembly via Cdc42 and N-WASP. Nat Cell Biol 2001;3:927–932. [PubMed: 11584276]

Jovic M, Kieken F, Naslavsky N, Sorgen PL, Caplan S. EHD1-associated Tubules Contain Phosphatidylinositol-4-Phosphate and Phosphatidylinositol-(4,5)-Bisphosphate and Are Required for Efficient Recycling. Mol Biol Cell. 2009

Jovic M, Naslavsky N, Rapaport D, Horowitz M, Caplan S. EHD1 regulates beta1 integrin endosomal transport: effects on focal adhesions, cell spreading and migration. J Cell Sci 2007;120:802–814. [PubMed: 17284518]

Kouranti I, Sachse M, Arouche N, Goud B, Echard A. Rab35 regulates an endocytic recycling pathway essential for the terminal steps of cytokinesis. Curr Biol 2006;16:1719–1725. [PubMed: 16950109]

Leonard D, Hayakawa A, Lawe D, Lambright D, Bellve KD, Standley C, Lifshitz LM, Fogarty KE, Corvera S. Sorting of EGF and transferrin at the plasma membrane and by cargo-specific signaling to EEA1-enriched endosomes. J Cell Sci 2008;121:3445–3458. [PubMed: 18827013]

Lichy JH, Modi WS, Seuanez HN, Howley PM. Identification of a human chromosome 11 gene which is differentially regulated in tumorigenic and nontumorigenic somatic cell hybrids of HeLa cells. Cell Growth Differ 1992;3:541–548. [PubMed: 1390339]

Lin SX, Grant B, Hirsh D, Maxfield FR. Rme-1 regulates the distribution and function of the endocytic recycling compartment in mammalian cells. Nat Cell Biol 2001;3:567–572. [PubMed: 11389441]

Magadan JG, Barbieri MA, Mesa R, Stahl PD, Mayorga LS. Rab22a regulates the sorting of transferrin to recycling endosomes. Mol Cell Biol 2006;26:2595–2614. [PubMed: 16537905]

Miserey-Lenkei S, Waharte F, Boulet A, Cuif MH, Tenza D, El Marjou A, Raposo G, Salamero J, Heliot L, Goud B, Monier S. Rab6-interacting protein 1 links Rab6 and Rab11 function. Traffic 2007;8:1385–1403. [PubMed: 17725553]

Naslavsky N, Boehm M, Backlund PS Jr, Caplan S. Rabenosyn-5 and EHD1 interact and sequentially regulate protein recycling to the plasma membrane. Mol Biol Cell 2004a;15:2410–2422. [PubMed: 15020713]

Naslavsky N, Weigert R, Donaldson JG. Convergence of non-clathrin- and clathrin-derived endosomes involves Arf6 inactivation and changes in phosphoinositides. Mol Biol Cell 2003;14:417–431. [PubMed: 12589044]

Naslavsky N, Weigert R, Donaldson JG. Characterization of a nonclathrin endocytic pathway: membrane cargo and lipid requirements. Mol Biol Cell 2004b;15:3542–3552. [PubMed: 15146059]

Nielsen E, Severin F, Backer JM, Hyman AA, Zerial M. Rab5 regulates motility of early endosomes on microtubules. Nat Cell Biol 1999;1:376–382. [PubMed: 10559966]

Niwa S, Tanaka Y, Hirokawa N. KIF1Bbeta- and KIF1A-mediated axonal transport of presynaptic regulator Rab3 occurs in a GTP-dependent manner through DENN/MADD. Nat Cell Biol 2008;10:1269–1279. [PubMed: 18849981]

Patino-Lopez G, Dong X, Ben-Aissa K, Bernot KM, Itoh T, Fukuda M, Kruhlak MJ, Samelson LE, Shaw S. Rab35 and its GAP EPI64C in T cells regulate receptor recycling and immunological synapse formation. J Biol Chem 2008;283:18323–18330. [PubMed: 18450757]

Powelka AM, Sun J, Li J, Gao M, Shaw LM, Sonnenberg A, Hsu VW. Stimulation-dependent recycling of integrin beta1 regulated by ARF6 and Rab11. Traffic 2004;5:20–36. [PubMed: 14675422]

Ritter B, Philie J, Girard M, Tung EC, Blondeau F, McPherson PS. Identification of a family of endocytic proteins that define a new alpha-adaptin ear-binding motif. EMBO Rep 2003;4:1089–1095. [PubMed: 14555962]

Sato M, Sato K, Liou W, Pant S, Harada A, Grant BD. Regulation of endocytic recycling by C. elegans Rab35 and its regulator RME-4, a coated-pit protein. Embo J 2008;27:1183–1196. [PubMed: 18354496]

Senderek J, Bergmann C, Weber S, Ketelsen UP, Schorle H, Rudnik-Schoneborn S, Buttner R, Buchheim E, Zerres K. Mutation of the SBF2 gene, encoding a novel member of the myotubularin family, in Charcot-Marie-Tooth neuropathy type 4B2/11p15. Hum Mol Genet 2003;12:349–356. [PubMed: 12554688]

Simonsen A, Lippe R, Christoforidis S, Gaullier JM, Brech A, Callaghan J, Toh BH, Murphy C, Zerial M, Stenmark H. EEA1 links PI(3)K function to Rab5 regulation of endosome fusion. Nature 1998;394:494–498. [PubMed: 9697774]

Simpson JC, Griffiths G, Wessling-Resnick M, Fransen JA, Bennett H, Jones AT. A role for the small GTPase Rab21 in the early endocytic pathway. J Cell Sci 2004;117:6297–6311. [PubMed: 15561770]

Sonnichsen B, De Renzis S, Nielsen E, Rietdorf J, Zerial M. Distinct membrane domains on endosomes in the recycling pathway visualized by multicolor imaging of Rab4, Rab5, and Rab11. J Cell Biol 2000;149:901–914. [PubMed: 10811830]

Thomas S, Ritter B, Verbich D, Sanson C, Bourbonniere L, McKinney RA, McPherson PS. Intersectin regulates dendritic spine development and somatodendritic endocytosis but not synaptic vesicle recycling in hippocampal neurons. J Biol Chem 2009;284:12410–12419. [PubMed: 19258322]

van der Sluijs P, Hull M, Webster P, Male P, Goud B, Mellman I. The small GTP-binding protein rab4 controls an early sorting event on the endocytic pathway. Cell 1992;70:729–740. [PubMed: 1516131]

Volterra A, Meldolesi J. Astrocytes, from brain glue to communication elements: the revolution continues. Nat Rev Neurosci 2005;6:626–640. [PubMed: 16025096]

Wada M, Nakanishi H, Satoh A, Hirano H, Obaishi H, Matsuura Y, Takai Y. Isolation and characterization of a GDP/GTP exchange protein specific for the Rab3 subfamily small G proteins. J Biol Chem 1997;272:3875–3878. [PubMed: 9020086]

Walseng E, Bakke O, Roche PA. Major histocompatibility complex class II-peptide complexes internalize using a clathrin- and dynamin-independent endocytosis pathway. J Biol Chem 2008;283:14717–14727. [PubMed: 18378669]

Weigert R, Yeung AC, Li J, Donaldson JG. Rab22a regulates the recycling of membrane proteins internalized independently of clathrin. Mol Biol Cell 2004;15:3758–3770. [PubMed: 15181155]

Zerial M, McBride H. Rab proteins as membrane organizers. Nat Rev Mol Cell Biol 2001;2:107–117. [PubMed: 11252952]

Zhang J, Fonovic M, Suyama K, Bogyo M, Scott MP. Rab35 controls actin bundling by recruiting fascin as an effector protein. Science 2009;325:1250–1254. [PubMed: 19729655]

Zhu H, Zhu G, Liu J, Liang Z, Zhang XC, Li G. Rabaptin-5-independent membrane targeting and Rab5 activation by Rabex-5 in the cell. Mol Biol Cell 2007;18:4119–4128. [PubMed: 17699593]

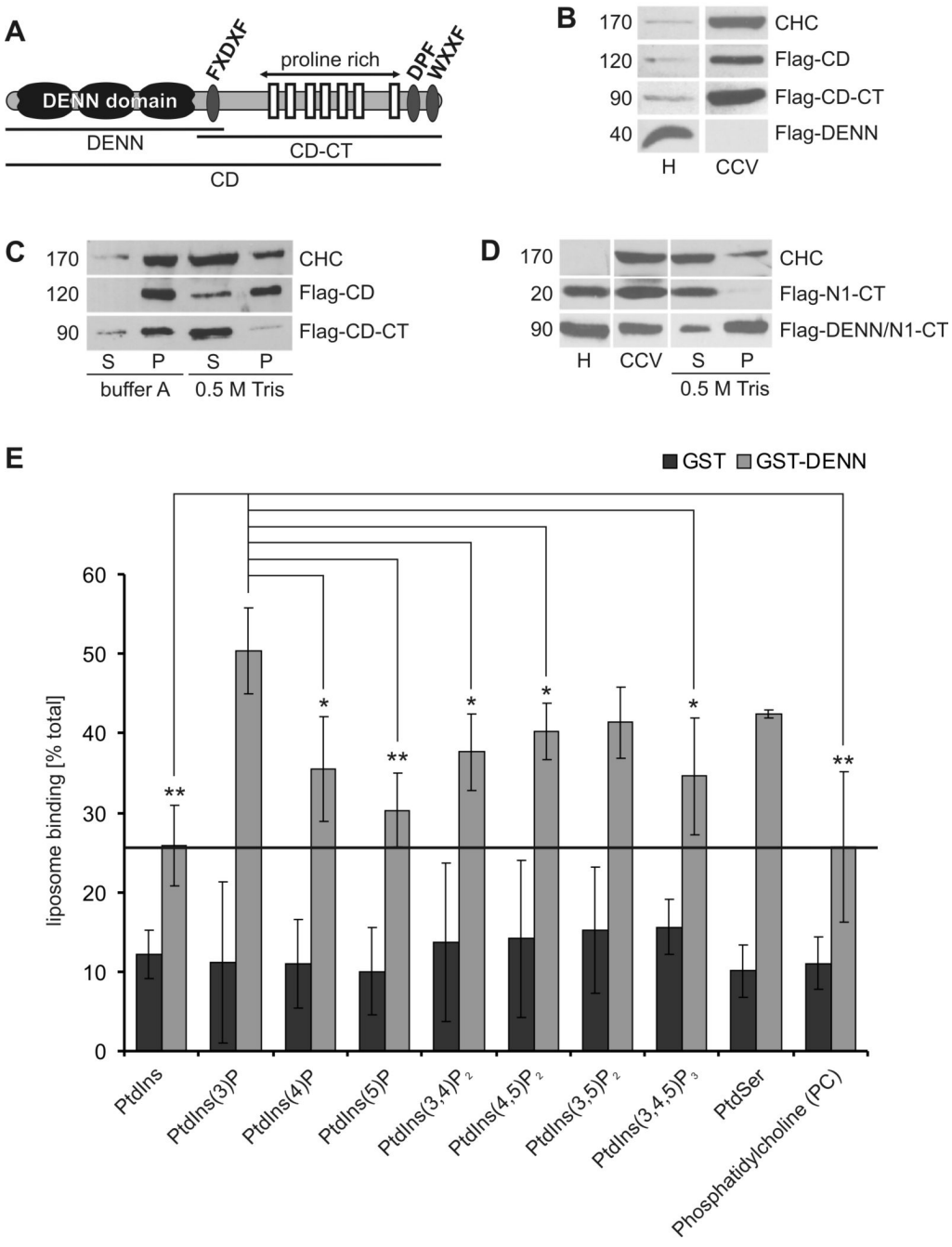

Figure 1. The connecdenn DENN domain binds lipids and is stably associated with membranes

A. Schematic representation of connecdenn (CD) indicating peptide motifs binding AP-2 (FXDXF, DPF, WXXF) and SH3 domain proteins (proline-rich) (Allaire et al., 2006). Borders of constructs used in the study are indicated **B**. Equal protein aliquots of homogenate (H) and CCVs isolated from HEK 293-T cells transfected with the indicated Flag-tagged connecdenn (CD) constructs were blotted with antibodies against clathrin heavy chain (CHC) and Flag. **C**. Equal amounts of CCVs isolated from cells expressing the indicated constructs were incubated with control buffer A or a Tris buffer to strip clathrin coats and the coat (supernatant, S) and vesicle (pellet, P) fractions generated by centrifugation were analyzed by Western blot, using CHC as control. **D**. Equal protein aliquots of homogenate (H) and CCVs isolated cells

expressing Flag-tagged C-terminal region of NECAP 1 (Flag-N1-CT) or a chimeric protein, where the connecdenn DENN domain had been fused to the NECAP 1 C-terminal region (Flag-DENN/N1-CT) were probed by Western blot with Flag and CHC antibodies along with coat (S) and vesicle (P) fractions prepared as described in C. **E**. Purified GST or GST-DENN domain were incubated with liposome suspensions (1 mg/ml) containing 90 mol% of PtdChol (PC) and 10 mol% of the indicated phospholipids. The bars represent the mean percentage (±STDEV) of starting material retained on liposomes, N=5. Paired T-tests revealed significant differences for DENN domain binding to PtdIns(3)P compared to the other lipids as indicated (* $p<0.05$, ** $p<0.01$). See also Fig. S1.

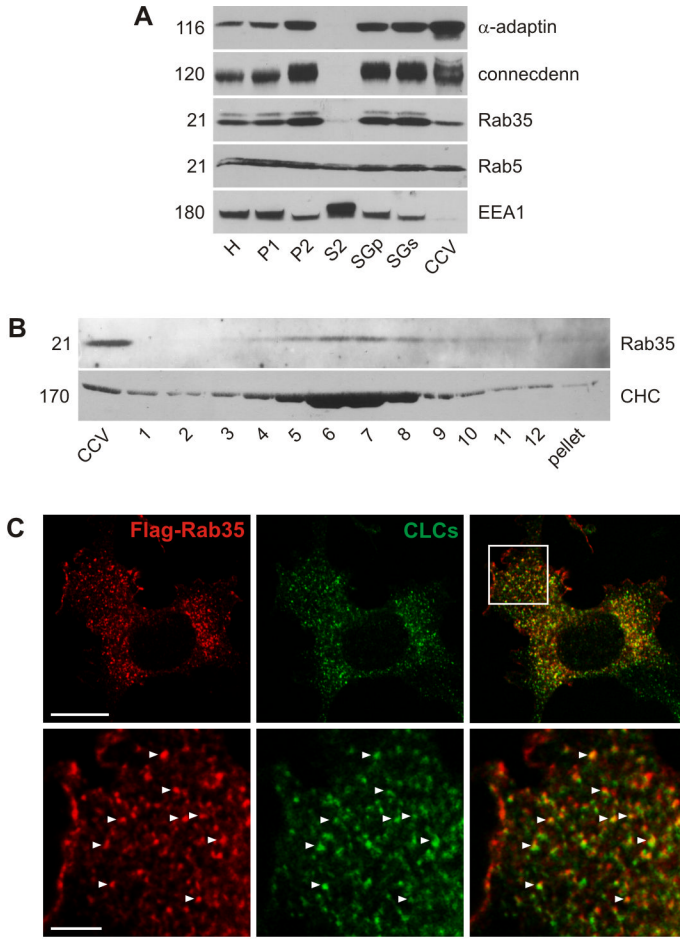

Figure 2. Rab35 is associated with CCVs

A. Equal protein aliquots of various fractions obtained during the purification of CCVs from adult rat brain were analyzed by Western blot for the indicated proteins. **B**. Purified CCVs were separated on a continuous sucrose gradient and aliquots of the gradient fractions were analyzed by Western blot with the indicated antibodies. **C**. COS-7 cells were transfected with Flag-Rab35 and the localization of Rab35 was compared to endogenous clathrin light chains (CLCs). The higher magnification shows the area highlighted by the box. Bar: 20 μm (low mag.), 5 μm (high mag.).

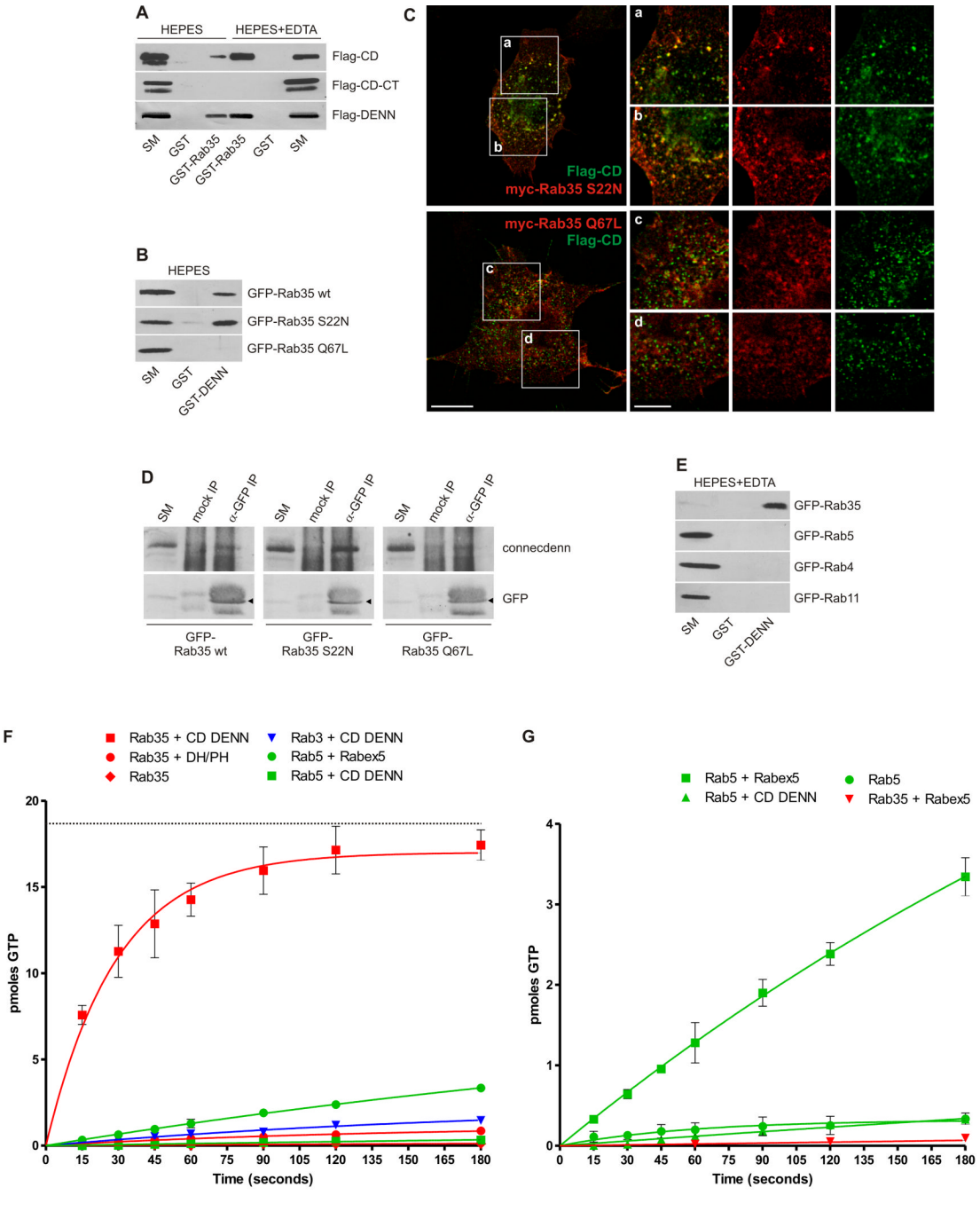

Figure 3. The connecdenn DENN domain binds Rab35 and functions as a GEF

A. Purified GST or GST-Rab35 were used to affinity-select Flag-tagged full-length connecdenn (CD), the C-terminal region (CD-CT) or the isolated DENN domain. Binding was performed in HEPES buffer alone or in the presence of 10 mM EDTA (HEPES+EDTA), which renders GTPases nucleotide-free, and interactions were detected by Western blot. **B**. Purified GST and GST-DENN domain were used to affinity-select the indicated GFP-tagged Rab35 constructs. Binding was revealed by GFP Western blot. For **A** and **B**, starting material (SM) equals 10% of the material used in each condition. **C**. COS-7 cells were transfected with Flag-tagged connecdenn (Flag-CD) and myc-tagged Rab35 S22N or Q67L and processed for immunofluorescence using antibodies directed against the tags. The regions highlighted by

boxes **a-d** are shown in higher magnification. Bar: 20 μm (low mag.), 5 μm (insets **a-d**). **D**. HEK 293-T cells were transfected with GFP-tagged Rab35 wt, S22N, and Q67L. Cell lysates were incubated with protein A-agarose alone (mock IP) or protein A-agarose with anti-GFP antibody (GFP IP). Specifically bound proteins were detected by blot with anti-GFP antibody or antibody recognizing endogenous connecdenn. The positions of the GFP-tagged Rab35 variants is indicated by the arrowheads. **E**. Purified GST and GST-DENN domain were incubated with lysates from HEK 293-T cells transfected with the indicated GFP-tagged Rabs and prepared under nucleotide-free conditions (HEPES+EDTA). Binding was revealed by Western blot using GFP antibodies. For **D** and **E**, starting material (SM) equals 10% of the material added to the beads. **F/G**. To measure GEF activity, 18.7 pmoles of GDP-loaded Rab3, Rab5, or Rab35 were incubated with 1.5 pmoles of connecdenn DENN domain, Rabex5 (aa1-399), or DH/PH domain of intersectin 1-l, a specific GEF for Cdc42, in the presence of 5 μM cold GTPγS and 0.2 mCi/mol ^{35}S-GTPγS. At the time points indicated, an aliquot of the reaction was analyzed for nucleotide exchange as described in the Experimental Procedures. pmoles of GTP exchanged are plotted over time (in seconds) and points represent mean (±STDEV), N=3. The curve was fit by nonlinear regression one phase association. The dotted line in **F** represents the total amount in pmole of Rab35 present in the reaction.

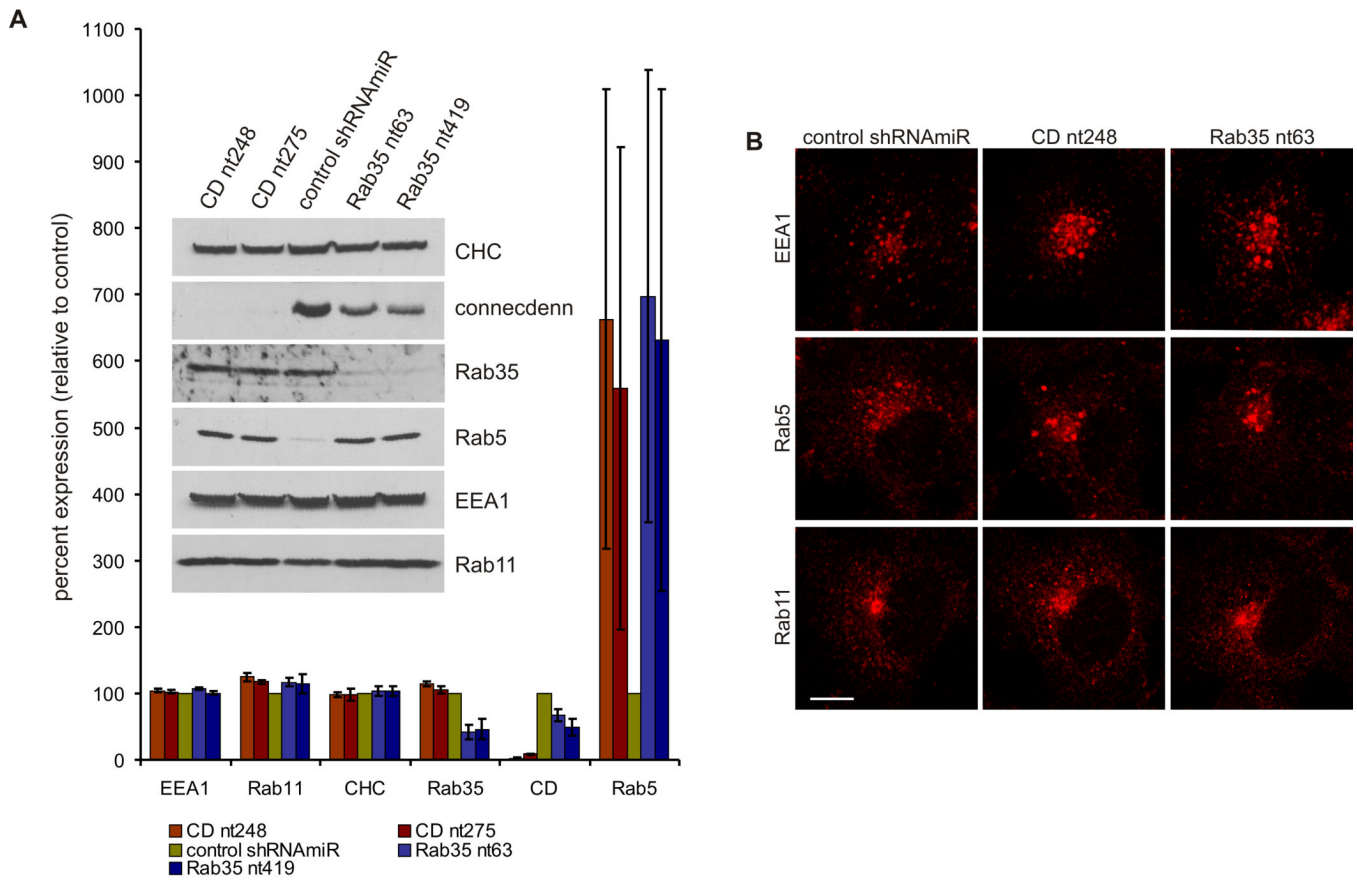

Figure 4. Connecdenn or Rab35 KD causes perinuclear clustering and enlargement of early endosomes

A. Equal aliquots of lysates from COS-7 cells transduced with control shRNAmiR or shRNAmiRs for KD of connecdenn (CD nt248 and CD nt275) or Rab35 (Rab35 nt63 and Rab35 nt419) were analyzed by Western Blot for the expression levels of the indicated proteins. For the bar graph, Western blots from four independent transductions were quantified by densitometry using ImageJ. Expression levels are represented in percent (±STDEV), setting the control shRNAmiR to 100%. **B**. Control and KD COS-7 cells were processed for immunofluorescence to reveal the localization of endogenous markers of early endosomes (EEA1, Rab5) and the recycling endosome (Rab11). Bar: 10 μm. See also Fig. S2.

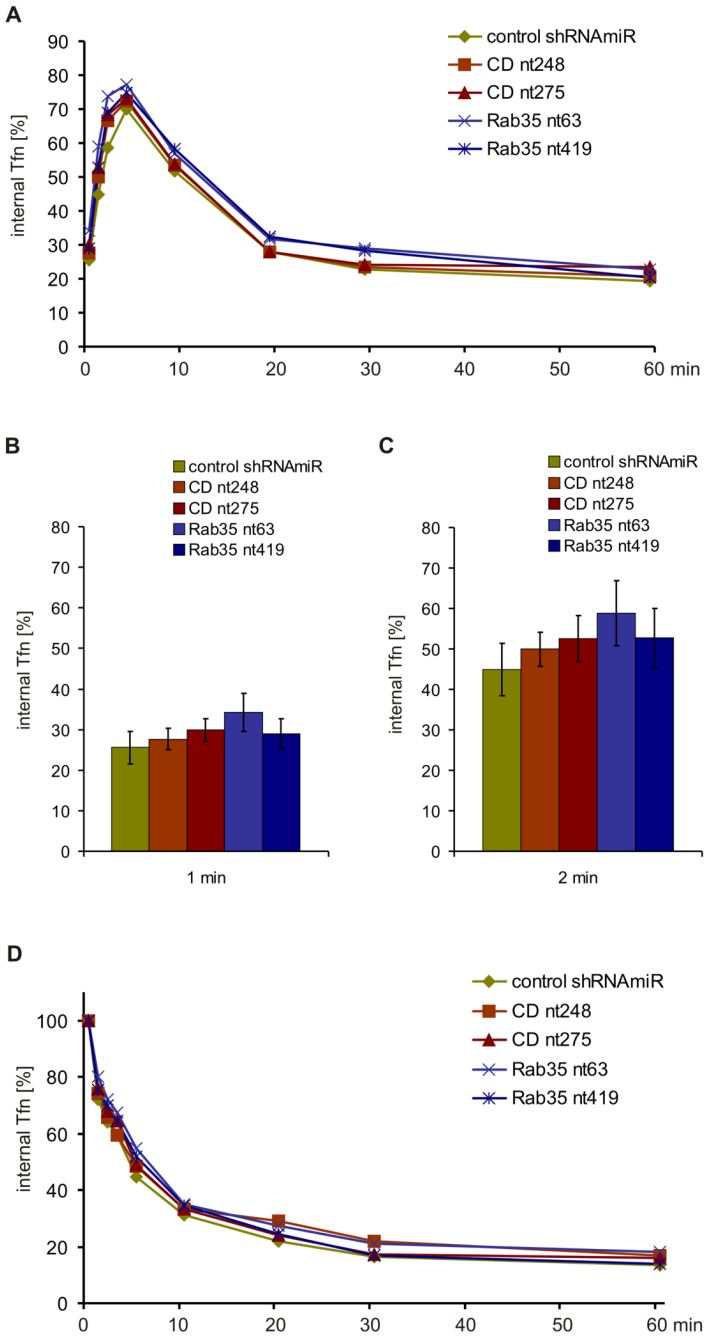

Figure 5. Connecdenn and Rab35 do not control transferrin trafficking

A. Control and KD COS-7 cells were surface-labeled on ice with AlexaFluor647-transferrin, shifted to 37°C for the indicated times, and intracellular transferrin was measured by flow cytometry. The graph represent the mean of percentage of the initial surface label (N=4) and statistical analysis by Repeated Measure Two-Way ANOVA followed by Bonferroni posttests revealed no significant differences between control and KD cells. **B**/**C**. The data for the 1 min (**B**) and 2 min time points (**C**) from panel (**A**) were replotted as bar graphs to highlight the lack of any endocytic defect (note the overlap in error bars for the different conditions). **D**. Control and KD COS-7 cells were continuously labeled with AlexaFluor647-transferrin at 37°C for one hour, chased at 37°C for the indicated times, and intracellular transferrin was measured

by flow cytometry. The graph represent the mean of percentage of the initial surface label (N=4) and statistical analysis by Repeated Measure Two-Way ANOVA followed by Bonferroni posttests revealed no significant differences between control and KD cells. See also Fig. S3.

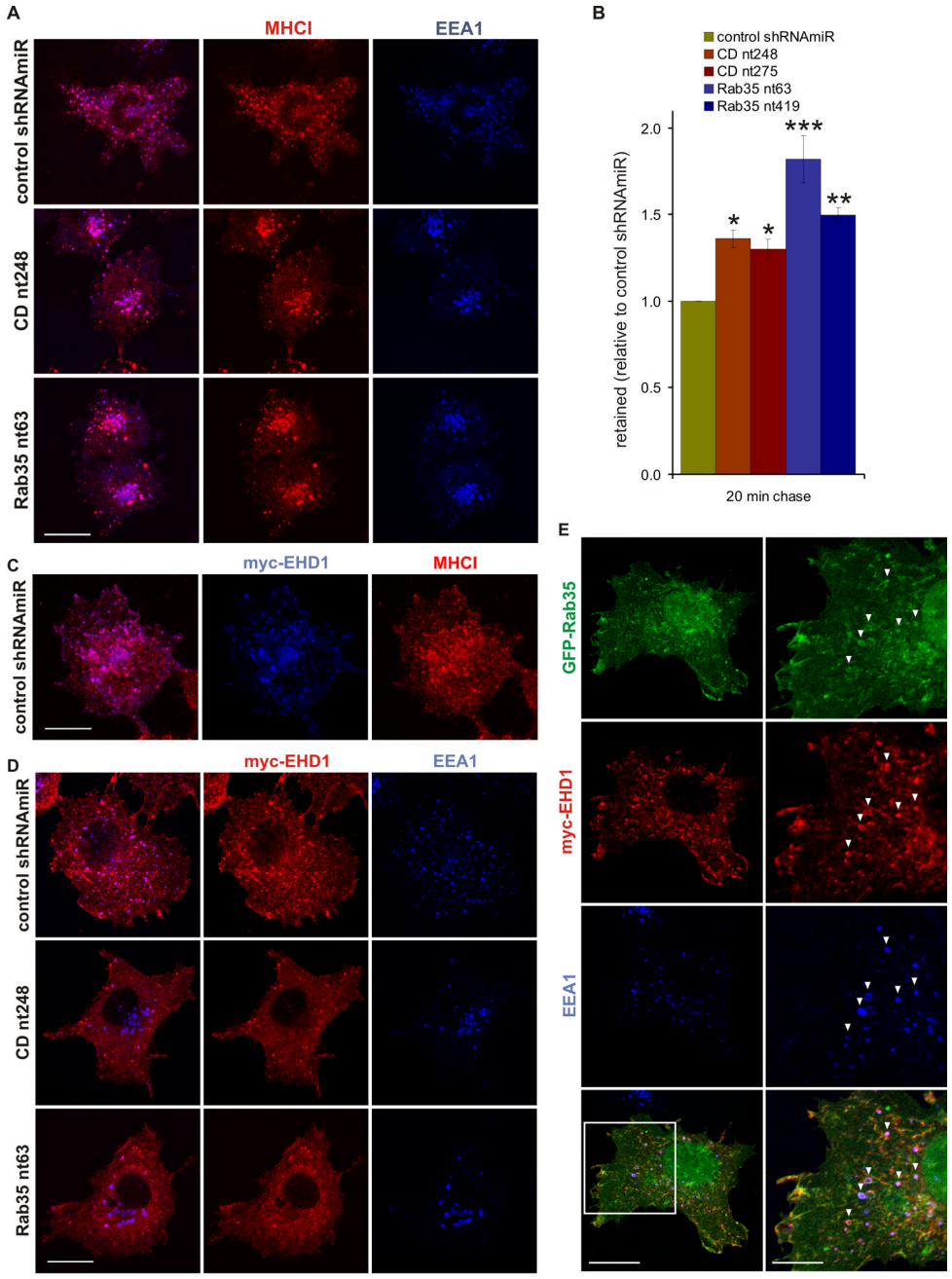

Figure 6. Connecdenn and Rab35 KD affects MHCI trafficking and EHD1 recruitment

A. Control and KD COS-7 cells were incubated for 20 min with antibodies against MHCI and processed by immunofluorescence to reveal the localization of the internalized antibodies and endogenous EEA1. Bar: 20 μm. **B**. Control and KD COS-7 cells were incubated for 20 min with antibodies against MHCI, chased for 20 min, and intracellular MHCI antibodies were detected by flow cytometry. The graph represent the mean fluorescence after the 20 min chase (N=4), plotted as relative ratio (±SEM) with the control shRNAmiR set to 1. Statistical analysis by Repeated Measure One-Way ANOVA followed by Dunnett's posttests revealed significant differences between control and KD cells (* $p<0.05$, ** $p<0.01$, *** $p<0.001$). **C**. COS-7 cells transduced with lentivirus for the expression of control shRNAmiR and transfected with myc-

EHD1 were incubated with antibodies against MHCI for twenty minutes and processed by immunofluorescence. Bar: 20 μm. **D**. Control and KD COS-7 were transfected with myc-EHD1 and processed by immunofluorescence to reveal the localization of EHD1 and endogenous EEA1. Bar: 20 μm. **E**. COS-7 cells transfected with expression constructs for GFP-tagged Rab35 and myc-tagged EHD1 were processed by immunofluorescence to reveal the localization of Rab35, EHD1, and endogenous EEA1. The arrowheads indicate areas of co-localization of all three proteins and the area highlighted by the box is shown in higher magnification. Bar: 20 μm (low mag.), 10 μm (high mag.). See also Fig. S4/S5.

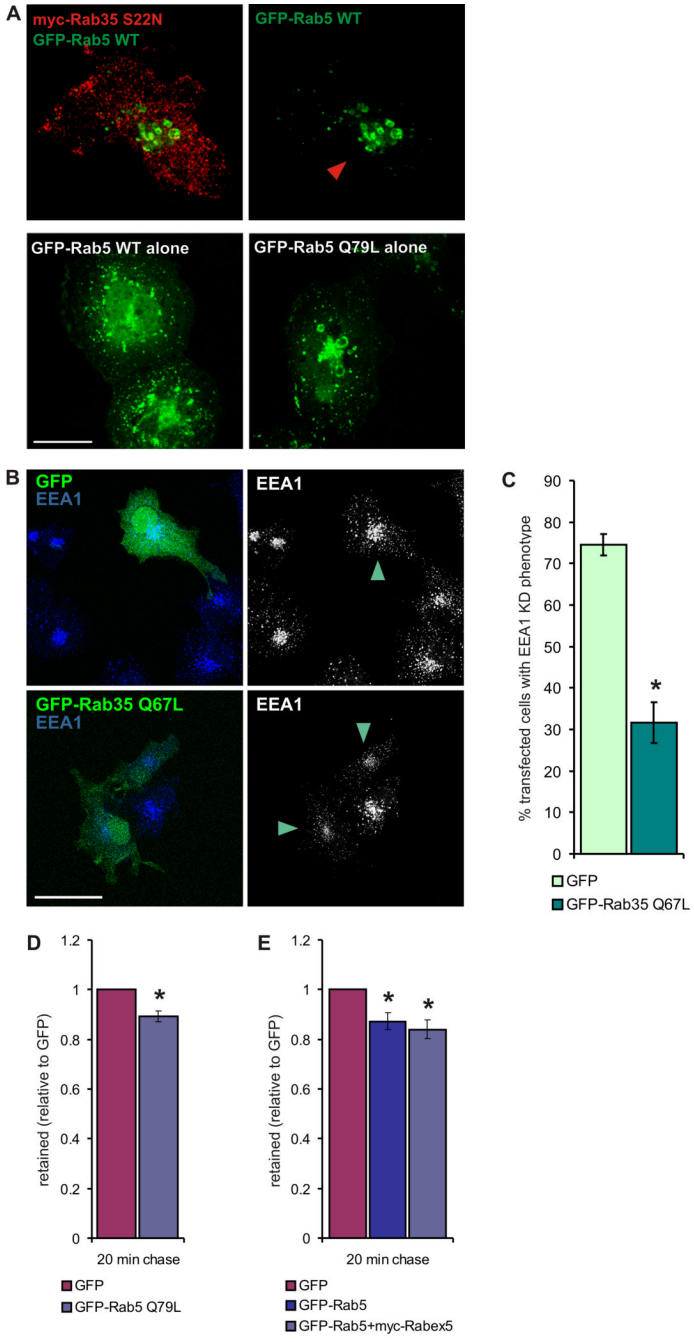

Figure 7. Loss of Rab35 activity causes the KD phenotypes

A. COS-7 cells were transfected with GFP-Rab5 wt or GFP-Rab5 Q67L alone, or co-transfected with GFP-Rab5 wt and myc-Rab35 S22N and processed by immunofluorescence to compare the effect of inactive Rab35 on the localization of Rab5. The arrowhead indicates the transfected cell when only the Rab5 signal is shown. Bar: 20 μm. **B**. Connecdenn KD cells (CD nt248) were transfected with GFP alone or GFP-tagged Rab35 Q67L and processed by immunofluorescence for endogenous EEA1 to reveal the localization and morphology of the early endosomal compartment. Arrowheads indicate the transfected cells when only the EEA1 signal is shown. Bar: 40 μm. **C**. Quantification of (**B**). The bar graph represents the mean percentage (±SEM, N=4) of transfected cells showing the EEA1 KD phenotype in connecdenn

KD cells expressing GFP alone or GFP-Rab35 Q67L. Statistical analysis by two-tailed Mann Whitney test revealed a significant difference between GFP- and GFP-Rab35 Q67L-expressing cells (* $p<0.05$). **D**. COS-7 cells transfected with GFP alone or with GFP-tagged Rab5 Q79L were incubated for 20 min with antibodies against MHCI, chased for 20 min, and intracellular MHCI antibodies were detected by flow cytometry. The graph represent the mean fluorescence after the 20 min chase (N=4), plotted as relative ratio (±SEM) with GFP set to 1. Statistical analysis by two-tailed T-test revealed a significant difference between GFP and GFP-Rab5 Q79L-expressing cells (* $p<0.05$). **E**. COS-7 cells transfected with GFP or GFP-Rab5 alone or co-transfected with GFP-Rab5 and myc-tagged Rabex5 were processed as described for (**D**). The graph represent the mean fluorescence after the 20 min chase (N=4), plotted as relative ratio (±SEM) with GFP set to 1. Statistical analysis by Repeated Measure One-Way ANOVA followed by Dunnett's posttests revealed significant differences between GFP and Rab5 or Rab5+Rabex5-expressing cells (* $p<0.05$).